CLOUD FRACTION STATISTICS DERIVED FROM 2-YEARS OF HIGH SPECTRAL RESOLUTION LIDAR DATA ACQUIRED AT EUREKA, CANADA.

Edwin W. Eloranta[1], Joseph P. Garcia[1], Igor A Razenkov[1], Taneil Uttal[2], Matthew Shupe[3]

[1]*University of Wisconsin, 1225 W. Dayton St, Madison,WI, 53706,USA, eloranta@lidar.ssec.wisc.edu*

[2]*NOAA-Earth System Research Laboratory, Complete mailing address(including country), taniel.uttal@noaa.gov*

[2]*NOAA and Cooperative Institute for Research in Environmental Science,325 Broadway, Boulder, CO,80305, USA, matthew.shupe@noaa.gov*

ABSTRACT

The Canadian Network for the Detection of Atmospheric Change (CANDAC) and the NOAA Study of Environmental Arctic Change (SEARCH) have installed instrumentation at Eureka(80 deg N, 86 deg W) in the Nunavut territory of Northern Canada. These instruments include the University of Wisconsin Arctic High Spectral Resolution Lidar(AHSRL) and the NOAA 8.6 mm wavelength cloud radar (MMCR). Both instruments have operated nearly continuously since Sept 2005.

This paper presents a record of cloud cover, cloud altitude and cloud phase derived from the lidar. It also presents comparisons between lidar, radar, and convention meteorological observations of cloudiness. It is shown that optically thin clouds are frequently observed at this site. As a result, the observed fractional cloud cover depends strongly on the optical depth threshold used to define the presence of cloud.

1. INTRODUCTION

Measurements show that Arctic is warming faster than the rest of the globe. Warming is also predicted by climate models. However, there is more disagreement between the predictions of individual models in the Arctic then at lower latitudes. Differences in cloud parametrization are the likely to be the main source of the model-to-model variations. Unfortunately, it is difficult to evaluate model predictions of Arctic cloudiness because of a lack of reliable cloud observations. Furthermore, cloudiness is often reported as fractional cloud cover without reference to cloud opacity. This produces an additional source of uncertainty that is particularly severe in the Arctic were clouds are often optically thin.

In this paper use we use high spectral resolution lidar and millimeter wavelength cloud radar data to measure cloud fraction and to illustrate the dependence of cloud fraction on the threshold used to define cloud presence.

The Canadian Network for the Detection of Atmospheric Change (CANDAC) and the NOAA Study of Environmental Arctic Change (SEARCH) have installed instrumentation at Eureka(80 deg N, 86 deg W) in the Nunavut territory of Northern Canada. These instruments include the University of Wisconsin Arctic High Spectral Resolution Lidar(AHSRL) and the NOAA 8.6 mm wavelength cloud radar (MMCR). Both instruments have operated nearly continuously since Sept 2005. Figure 1 shows a monthly record of AHSRL operation. The lidar has been successful in acquiring data approximately 90% of the time. Only laser malfunctions in August of 2006 and April-May 2007 provided serious data gaps. All of the data used in this study can be viewed and downloaded from the web site: http://lidar.ssec.wisc.edu.

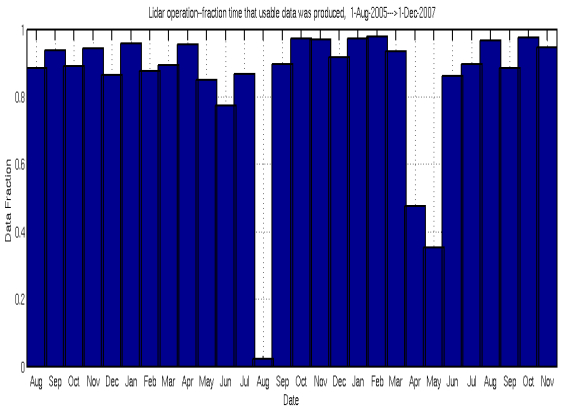

Figure 1: AHSRL operation record a Eureka from 2-August-2005 through 1-December-2007. Data gaps in August 2006 and Apr-May 2007 were cause by laser failures that required trips to Eureka.

2. CLOUD DETECTION

The AHSRL[1] provides absolutely calibrated measurements of backscatter cross section, optical depth and depolarization at a wavelength of 532nm. The AHSRL avoids the ambiguities which result from unstable inversions and assumptions about the nature of the scattering media which must be invoked to correct standard backscatter lidar measurements for attenuation.

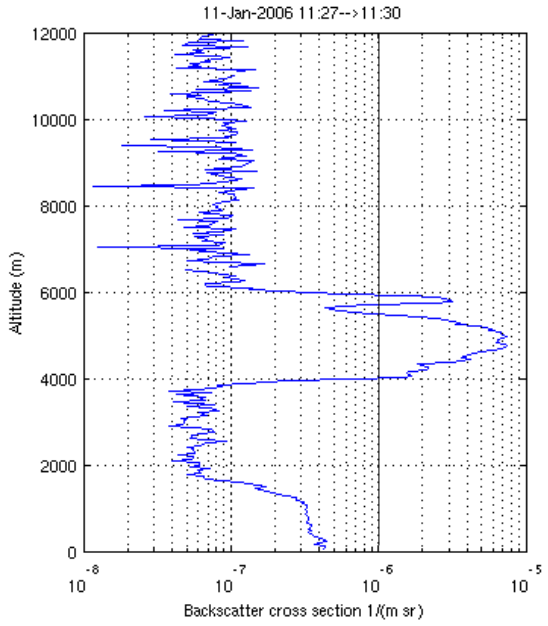

Figure 2. A typical AHSRL backscatter cross section profile recorded between 11:27 and 11:30 UT on 11-Jan-06 with a dark line at a backscatter cross section of 1e-6 m^{-1} sr^{-1}.

Our cloud detection algorithm works by searching for a cloud base. AHSRL signals, which are acquired with 2.5 second and 7.5 m time and altitude averages, are first averaged to 3 min and 45 m resolutions. This improves signal to noise and reduces nearly 0.5 terabyte of data in the raw files to a more manageable volume. Because the HSRL calibration is depend on normalization by the molecular backscatter signal, a molecular signal strength mask is applied to eliminate profile segments above dense clouds where the molecular signal is attenuated. In this study we have masked signals where fewer than 70 photons have been detected in a 3 min, 45 m range bin.

We choose to state our cloud detection threshold in terms of optical depth, because of its fundamental role in determining the radiative effect of a cloud. However, instead of directly applying the optical depth threshold we begin by requiring that the backscatter cross section exceed a threshold value within a cloud. This is necessary because small fluctuations in the AHSRL overlap function cause small variations in the optical depth at low altitudes (typically OD ~0.05 below ~ 1km). These would cause false cloud detections at low altitudes.

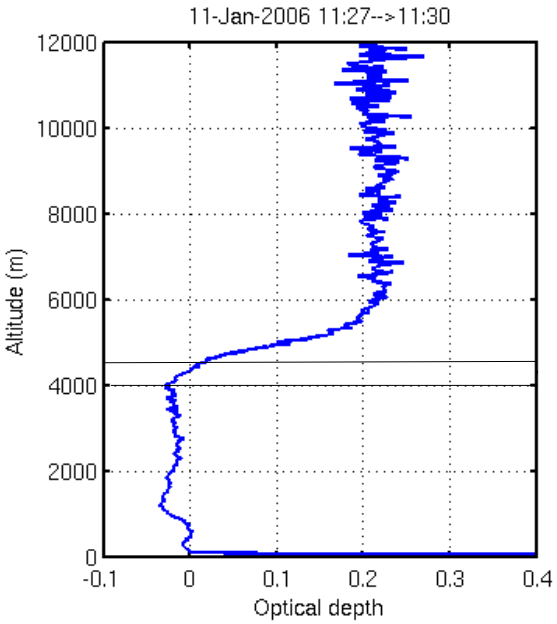

Figure 3. Optical depth vs altitude for data shown in figure 2. Notice the negative excursion of the optical depth at low altitudes caused by fluctuations in the lidar overlap function.. By integrating optical depth starting at the backscatter cloud base(4km) the until the threshold (OD=0.03) is reached at an altitude of ~4.3 km the algorithm avoids most of the error produced by overlap fluctuations.

The AHSRL backscatter cross section is a ratio measurement and is not subject to errors in the overlap correction. Thus, by setting a threshold on backscatter we can ensure that aerosol, haze, precipitation or cloud particles are present. This threshold is typically set at

1.0e-6 m^{-1} sr^{-1} insuring that even tenuous clouds are included (For reference the Rayleigh molecular backscatter cross section at the earths surface is ~1.6e-6 m^{-1} sr^{-1}). Figure 2 shows a typical backscatter profile with a low altitude cloud. Notice that a backscatter threshold of 1.0e-6 m^{-1} sr^{-1} of easily detects the cloud between 4 and 6 km without detecting the boundary layer aerosol below 2 km. Our cloud base algorithm begins integrating the optical depth from the base of the backscatter detected cloud. Cloud base then occurs when the integrated optical depth reaches the OD threshold.

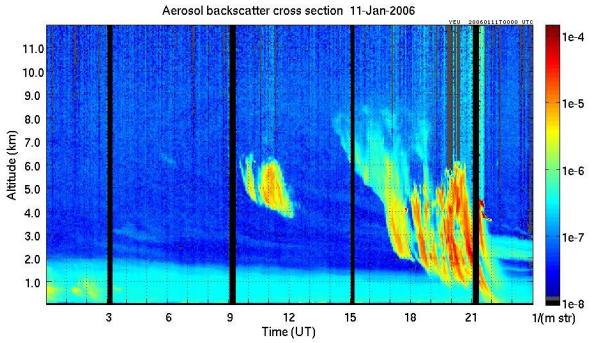

Figure 4. Lidar backscatter cross section for 11-Jan-06.

Depolarization measurements show that the mid-level clouds patches starting at 9:30 and 14:30 UT are predominately ice clouds with only small pockets of water at ~19 and ~21:30 UT at ~4km altitude. A relatively dense water haze layer is present between 19 and 24 UT between 2 and 3km while a boundary layer haze layer is present below 2km.

Figure 5 shows the the image presented in figure 4 along with cloud thresholds derived by lidar and radar.

Radar cloud boundaries were based on a backscatter cross section of 1e-15 m^{-1} sr^{-1} (reflectivity = -66 dBz).

Examination of many images with superimposed cloud boundaries shows the expected behavior. The radar is very sensitive to clouds and precipitation consisting of large ice crystals although it often fails to detect small ice crystals in high cold cirrus and thin water clouds composed of small water droplets. While the lidar using backscatter thresholds is apt to trigger on optically thin haze layers.

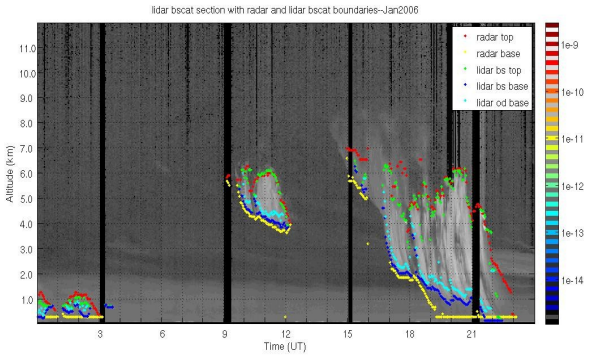

Figure 5. Lidar backscatter cross section with cloud boundaries detected by lidar and radar.

The lowest cloud bases in figure 5 are reported by the radar which is very sensitive to large diameter ice crystals. The second lowest cloud base is reported by lidar using a backscatter cross section threshold of 1e-6 m^{-1} sr^{-1} and the highest base shown in this plot generated using an optical depth threshold. An optical depth threshold of 0.03 was used in this example. This is commonly used as an approximate threshold to distinguish between sub-visible and visible clouds.

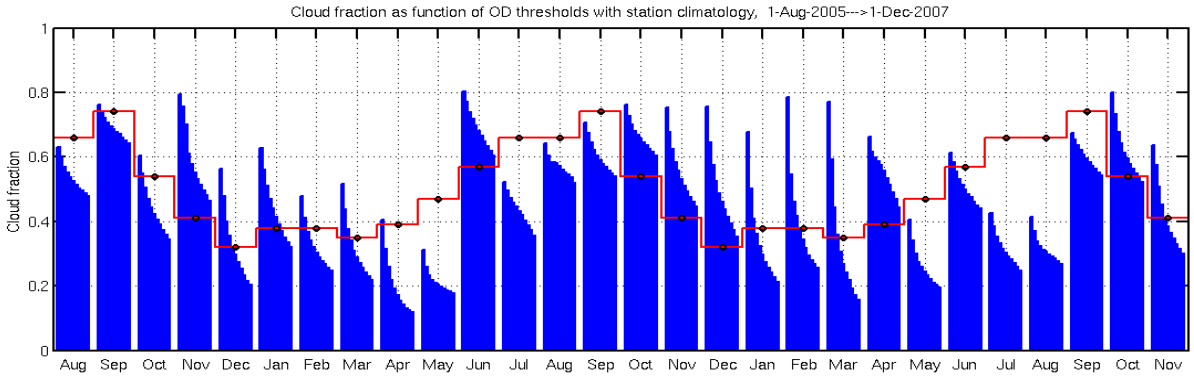

Figure 6: AHSRL monthly cloud fractions for Eureka.

3. CLOUD STATISICS

Figure 6 shows cloud fractions derived for Eureka using the high spectral resolution lidar and cloud fractions derived from a conventional climatology prepared by Vowinkel[2]. The lidar cloud fraction is plotted by month and by optical depth threshold as a series of bar graphs with the left-most bar of each month computed for and optical depth threshold of 0.03 and the second bar for a threshold of 0.1 with the threshold increasing by 0.1 for each successive bar until the right-most bar represents an optical depth threshold of 1.0. Notice that the observed cloud fraction is highly dependent on the choice of threshold. This is particularly true during the winter months when clouds are predominately composed of ice and are optically very thin.

When cloud fractions are plotted vs optical depth threshold in figure 7 the seasonal dependence of cloud fraction is clearly evident. Summer months which have more water clouds show a smaller threshold dependence than winter months where optically thin ice clouds are prevalent.

comparison between lidar and radar optical depths shows expected strong dependence on particle size indicating that the radar signature is not a good indicator of cloud optical properties.

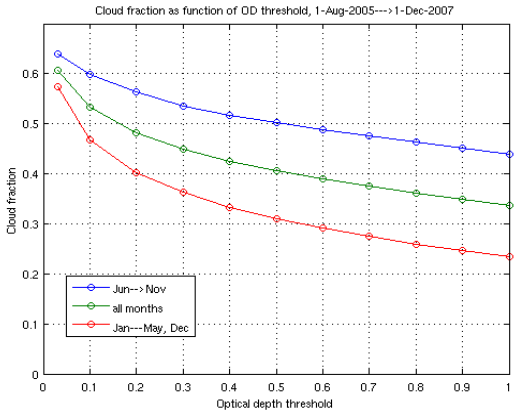

Figure 7. Lidar cloud fraction as a function of optical depth threshold by seasons.

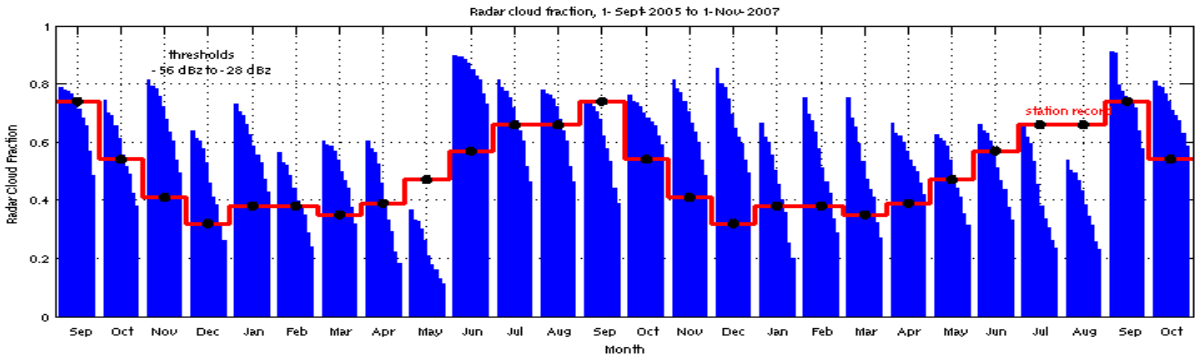

Figure 8. Monthly cloud fraction as a function of radar reflectivity.

Figure 8 shows monthly cloud fractions as seen by the the MMCR radar as a function of the radar reflectivity. Radar thresholds range from -56dBz on left to -20 dBz on the right side of each monthly bar. The conventional climatology of Vowinkel and Orvig[2] is plotted as a solid line. Once again cloudiness is a strong function of threshold. Comparisons of the lidar and radar cloud fractions with the Vowinkel and Orvig climatology show best fits with a lidar optical depth threshold of 0.25 and with a radar threshold of -26dBz. A

4. ACKNOWLEDGMENTS

This research was supported by NOAA contract RA133R07-07-SE-2465, National Science Foundation grant ARC-0612452 and DOE Grant DE-FG02-06ER64187.

REFERENCES

[1]Eloranta, E. W.: High Spectral Resolution Lidar, *in Lidar:Range-Resolved Optical Remote Sensing of the Atomsphere,* Klaus Weitkamp ed., Springer, NY.

[2]Vowinkel and Orvig: World Survey of Climatology, **14**, p127-152, 1970